

# Experimental Synchronization in Coupled Spatially Extended Systems

Takao FUKUYAMA

*Faculty of Education, Ehime University, Bunkyo-cho 3, Matsuyama, Ehime 790-8577, JAPAN*

Yoichi WATANABE, and Yoshinobu KAWAI

*Interdisciplinary Graduate School of Engineering Sciences, Kyushu University,  
Kasugakoen 6-1, Kasuga, Fukuoka 816-8580, JAPAN*

(Received: 1 September 2008 / Accepted: 15 October 2008)

Synchronization between two unstable waves generated by current-driven ion-acoustic instability is observed experimentally, and the dynamical behavior of coupled systems is studied. When two spatially extended systems interact, and the dc potential applied to either of the two systems is varied gradually while maintaining coupling, the systems exhibit synchronization. Furthermore, it is found that the systems exhibit hysteresis phenomena around the threshold of synchronization.

Keywords: Chaos, Instability, Coupled Oscillators, Synchronization, Spatiotemporal Structure, Hysteresis

## 1. Introduction

Synchronization between oscillating systems is a universal phenomenon observed in nature; and its ancient roots were presented in the publication of Huygens's pendulum [1]. Recently, synchronization of not only periodic oscillators (limit cycle) but also chaotic oscillators, namely, chaos synchronization [2,3], was reported. Over the past decades, investigations on the synchronization of two chaotic oscillators have attracted considerable attention and have been reported in many branches of science [4-7]; these investigations were pioneered by Winfree, who investigated coupled nonlinear oscillators [8]. According to the characteristic property of coupled oscillators, two oscillators can be synchronized through a coupling interaction. The behavior of coupled oscillators is a phenomenon of interest in plasma physics so as to understand the interaction and coupling between various waves excited in plasma. Many types of waves whose analysis is essential from the viewpoint of nonlinear phenomena exist and propagate in plasma because of various instabilities in plasmas.

Plasma is a typical nonlinear dynamical system with large degrees of spatiotemporal freedom. Thus far, most investigations on coupled oscillators have been performed under the specified condition that each oscillator is a function that depends on only time, i.e., spatial freedom is not taken into account; however the spatiotemporal structure has recently attracted considerable attention [9-12]. Then, in spatially extended systems such as waves in plasma, an understanding in space and time is required. When the behavior of nonlinear wave-wave interaction in plasma is studied from the viewpoint of coupled nonlinear oscillators and each wave corresponds to an autonomous oscillator, it should be considered that each oscillator is a spatially extended system and has spatial freedom.

author's e-mail: fukuyama@ed.ehime-u.ac.jp

When synchronization occurs in coupled oscillators, the coupled systems exhibit various synchronized states such as lag synchronization [13], phase synchronization [14], and complete synchronization [2,3]. Lag synchronization implies synchronization in which two signals lock their phases and amplitudes but with a time lag. In phase synchronization, phases are locked while the amplitudes remain uncorrelated. Finally, complete synchronization implies synchronization in which there is a perfect hooking of the chaotic trajectories of two systems.

The behavior of coupled spatially extended systems, i.e. nonlinear wave-wave interaction in plasma, is investigated, and it is of interest to investigate different original phenomena that occur due to spatiotemporal nonlinearity in plasma in comparison with the universal characteristics of chaos. Previously, the authors have reported synchronization in coupled oscillators due to ion-acoustic instability [15], and contiguously-developed results are reported in this paper.

## 2. Experimental Setup and Excitation of Instability

Experiments are performed using a double-plasma device [16] with a diameter of 70 cm and length of 120 cm. The chamber of the device contains two cages composed of multipole permanent magnets for surface plasma confinement; tungsten filaments acting as cathodes are wound around the chamber wall. The chamber is divided at the center into two regions by a separation grid maintained at a floating potential. In this experiment, plasma is generated only in one region, which is the experimental region. The chamber is evacuated to  $4.0 \times 10^{-7}$  torr, and argon gas is introduced into the chamber at a pressure of  $4.0 \times 10^{-4}$  torr. Typical plasma parameters are as follows: electron density  $n_e \sim 10^8 \text{ cm}^{-3}$  and electron and ion

temperatures  $T_e \sim 0.5\text{--}1.0$  eV and  $T_i \sim T_e/(10\text{--}15)$ , respectively.

Current-driven ion-acoustic instability is excited by two parallel mesh grids  $G_1$  and  $G_2$  having the following dimensions: diameter 6.0 cm; grid 50 mesh/in; and interval  $L$  3.0 cm; these two grids are placed in a measurement system where dc potential is applied to either of them [17]. The instability is caused by the interaction between electron streaming, i.e., electron current, and background ion-acoustic waves in the plasma [18-23]. When dc potential is applied to either of the two mesh grids, an electric field is generated between them. Electrons are accelerated according to the generated electric field and the electron current flows between the two mesh grids. As mentioned above, instability occurs due to the interaction between this electron current and the background ion-acoustic waves in the plasma. When the biased grid potential exceeds a threshold, a current-driven ion-acoustic instability is excited and oscillations occur [17].

The dc potential  $V_m$  is applied to  $G_1$  and  $V_s$  is applied to  $G_2$ .  $V_m$  and  $V_s$  are control parameters that govern instability 1 and instability 2, respectively.  $V_s$  is fixed at 65 V and  $V_m$  is varied. It should be noted that unstable “traveling” waves are excited by instability 1 and instability 2; therefore, each wave is directly coupled by an interaction. Coupled spatially extended systems are schematically shown in Fig. 1. Time series signals for analysis are obtained from the fluctuating components of the currents on the biased mesh grids on both sides ( $G_1$ ,  $G_2$ ) and are sampled with a digital oscilloscope.

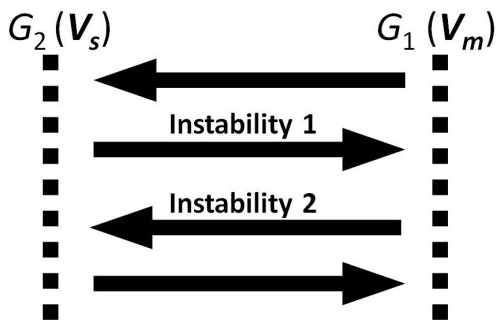


Fig. 1. Schematic of coupled spatially extended systems.

### 3. Results and Discussion

#### 3.1 Dynamical Behavior of Coupled Systems

The behavior of coupled spatially extended systems is investigated in the case that two oscillations caused by the current-driven ion-acoustic instability interact by a wave-wave interaction. The experiment consists of two processes explained in the following paragraphs.

First, the control parameter  $V_m$  is gradually increased while maintaining coupling and the behavior of the coupled systems is examined. Here, the control parameter

$V_s$  is fixed at 65 V, as mentioned before. The time series and  $X$ - $Y$  plot of the two instabilities are shown in Fig. 2. Left, middle, and right traces correspond to time series signals on  $G_1$ , time series signals on  $G_2$ ,  $X$ - $Y$  plot, respectively. For  $0 \text{ V} \leq V_m \leq 4 \text{ V}$ , only instability 2 oscillates since instability 1 is not yet excited in this range of  $V_m$ , as shown Fig. 2(a). For  $4 \text{ V} \leq V_m \leq 11 \text{ V}$ , instability 2 is suppressed slightly and the oscillation falls into disorder, as shown Fig. 2(b). For  $11 \text{ V} \leq V_m \leq 23 \text{ V}$ , the oscillation regains order, as shown in Fig. 2(c). For  $23 \text{ V} \leq V_m \leq 40 \text{ V}$ , instability 1 also begins to get excited and the two waves interact; thus, the wave resulting from instability 1 shows intermittency with burst oscillation. However, the two waves oscillate almost independently, and the coupled system does not attain the synchronization state, namely, non-synchronization, as shown in Fig. 2(d). For  $40 \text{ V} \leq V_m \leq 55 \text{ V}$ , the oscillation caused by instability 1 is suppressed and considerably smaller than that by instability 2, as shown in Fig. 2(e). For  $55 \text{ V} \leq V_m \leq 58 \text{ V}$ , the oscillation caused by instability 2 is also suppressed; therefore, coupled systems almost stops oscillating, as shown in Fig. 2(f). With increasing  $V_m$ , for  $58 \text{ V} \leq V_m \leq 65 \text{ V}$ , the oscillations of the two waves gradually increase again, as shown in Fig. 2(g). For  $65 \text{ V} \leq V_m \leq 100 \text{ V}$ , complete synchronization, which implies hooking of the chaotic trajectories of two systems, is observed in the coupled system, as shown in Fig. 2(h).

Second, the control parameter  $V_m$  is gradually decreased after being increased up to 100 V in the first experiment; coupling is maintained at this time, and the behavior of the coupled systems is examined. Here, the control parameter  $V_s$  is still maintained at 65 V. The time series and  $X$ - $Y$  plot of the two instabilities in this case are shown in Fig. 3. Left, middle, and right traces correspond to time series signals on  $G_1$ , time series signals on  $G_2$ ,  $X$ - $Y$  plot, respectively. For  $100 \text{ V} \geq V_m \geq 48 \text{ V}$ , complete synchronization is observed, as shown in Figs. 3(a) and (b). For  $53 \text{ V} \geq V_m \geq 48 \text{ V}$ , the amplitudes of coupled systems suddenly increase while maintaining complete synchronization, as shown in Fig. 3(b). With decreasing  $V_m$ , for  $48 \text{ V} \geq V_m \geq 46 \text{ V}$ , the shape of the  $X$ - $Y$  plot gradually changes from a straight line to an ellipse, as shown in Figs. 3(c) and (d). This implies that the complete synchronization in coupled systems changes to lag synchronization, in which two signals lock their phases and amplitudes but with a time lag, as mentioned earlier. For  $46 \text{ V} \geq V_m \geq 30 \text{ V}$ , the oscillation caused by instability 1 is suppressed and considerably smaller than that by instability 2, as shown in Fig. 3(e). The wave generated by instability 2 shows intermittency including burst oscillation, which is similar to the oscillation caused by instability 1, as shown in Fig. 2(d). For  $30 \text{ V} \geq V_m \geq 0 \text{ V}$ , only the oscillation caused by instability 2 are present since the oscillation caused by instability 1 almost disappears in this range of  $V_m$ , as shown Fig. 3(f).

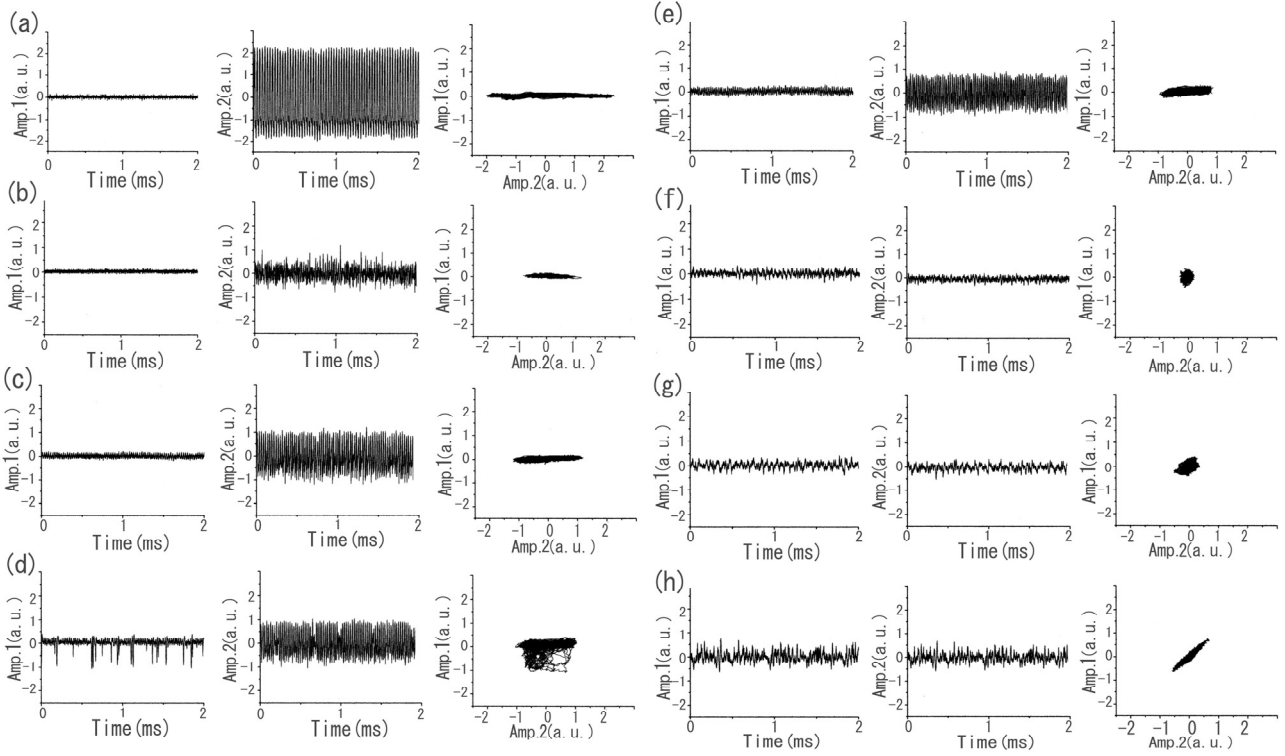


Fig. 2. The time series and  $X$ - $Y$  plot of the two instabilities are shown. Left, middle, and right traces correspond to time series signals on  $G_1$  ( $V_m$  is applied), time series signals on  $G_2$  ( $V_s$  is applied),  $X$ - $Y$  plot, respectively. The control parameter  $V_m$  is gradually increased. Here, the control parameter  $V_s$  is fixed at 65 V. (a)  $V_m = 0$  V, (b)  $V_m = 8$  V, (c)  $V_m = 20$  V, (d)  $V_m = 33$  V, (e)  $V_m = 45$  V, (f)  $V_m = 55$  V, (g)  $V_m = 60$  V, and (h)  $V_m = 85$  V.

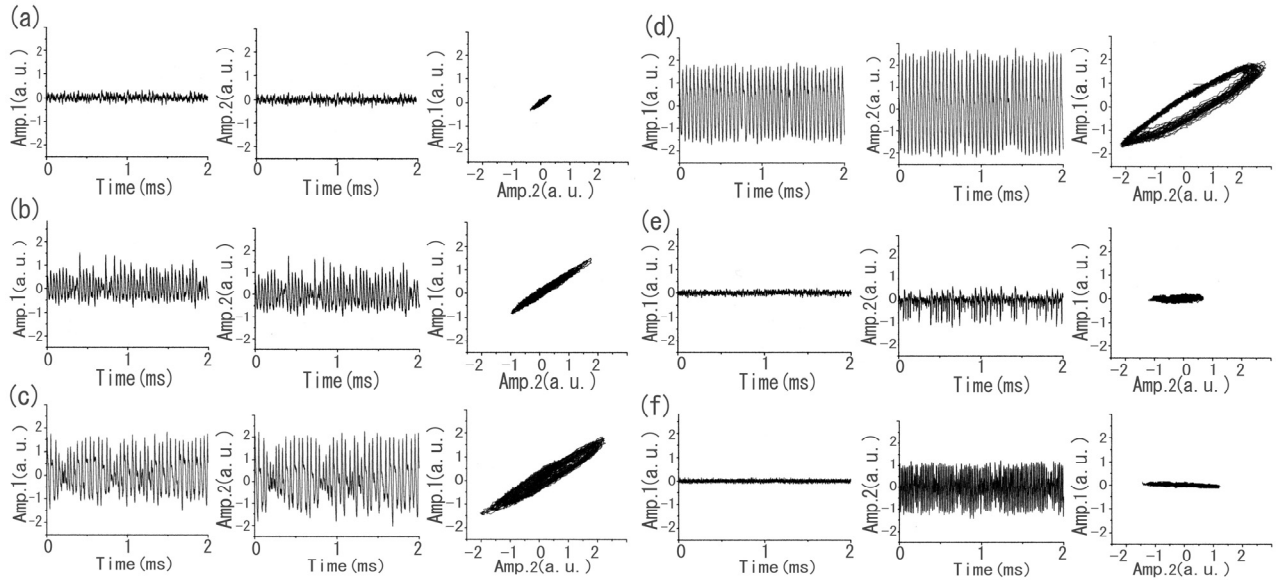


Fig. 3. The time series and  $X$ - $Y$  plot of the two instabilities are shown. Left, middle, and right traces correspond to time series signals on  $G_1$  ( $V_m$  is applied), time series signals on  $G_2$  ( $V_s$  is applied),  $X$ - $Y$  plot, respectively. The control parameter  $V_m$  is gradually decreased. Here, the control parameter  $V_s$  is fixed at 65 V. (a)  $V_m = 55$  V, (b)  $V_m = 50$  V, (c)  $V_m = 48$  V, (d)  $V_m = 47$  V, (e)  $V_m = 46$  V, and (f)  $V_m = 10$  V.

### 3.2 Hysteresis in Coupled Systems

The behavior of coupled systems is observed when  $V_s$  is fixed and  $V_m$  is varied. The observation results are listed in Table 1.  $V_m$  is first increased and then decreased; then, for any given value of  $V_m$ , the behaviors of the coupled

systems with an increase in this  $V_m$  value are different from those with a decrease in this value. This implies that the coupled systems exhibit hysteresis phenomena around the threshold of synchronization, as shown in Fig. 4. Such hysteresis phenomena related to synchronization barely

appear in coupled systems; that is, the behavior of a system is uniquely decided by an individual control parameter. Plasma is a medium with a strong self-nonlinearity because of large degrees of spatiotemporal freedom, and in most cases, phenomena occurring due to a control parameter should be considered as non-Markovian processes. A synchronized coupled system is almost steady, and the history of its stability is stored in plasma; therefore, hysteresis phenomena are observed.

Range (V)	Instability 1	Instability 2	State
$0 \leq V_m \leq 23$	Suppressed	Excited	No Synch.
$23 \leq V_m \leq 40$	Excited	Excited	No Synch.
$40 \leq V_m \leq 55$	Suppressed	Excited	No Synch.
$55 \leq V_m \leq 58$	Suppressed	Suppressed	No Oscillation
$58 \leq V_m \leq 100$	Excited	Excited	Synch.
$100 \geq V_m \geq 46$	Excited	Excited	Synch.
$46 \geq V_m \geq 0$	Suppressed	Excited	No Synch.

Table 1. The behavior of coupled systems is observed when  $V_s$  is fixed and  $V_m$  is varied. The observation results are listed.

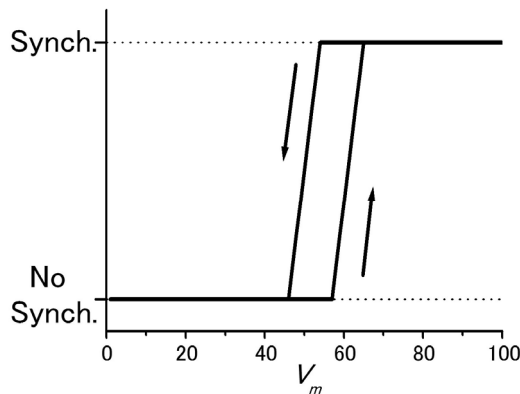


Fig. 4. Hysteresis phenomena around the threshold of synchronization are exhibited.

### 3.3 Correlation of Phase and Amplitude between Two Oscillators in Coupled Systems

When synchronization occurs in coupled oscillators, there exists a correlation between the phases of oscillations and a correlation between the amplitudes of these oscillations. Figures 5(a) and (b) show typical non-synchronized and synchronized states, respectively. The time series and  $X$ - $Y$  plot of the two instabilities are shown in this figure. Figures 6(a) and (b) show the phase difference  $|\phi_1 - \phi_2|$  and amplitude difference between two oscillators that are in a typical non-synchronized state. Sampled time series are analyzed using a low-pass filter that can pass frequencies of less than 100 kHz. Figure 6(a) shows that the phase difference increases with time.

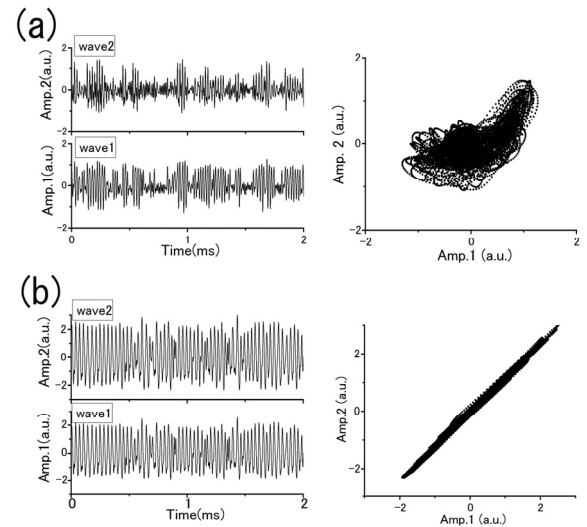


Fig. 5. The behavior of coupled systems is shown: (a) typical non-synchronized and (b) synchronized states. Left and right traces correspond to the time series and  $X$ - $Y$  plot of the two instabilities, respectively.

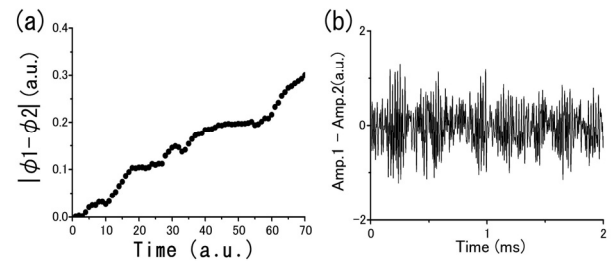


Fig. 6. Correlation between two oscillators is shown: (a) the phase difference  $|\phi_1 - \phi_2|$  and (b) amplitude difference between two oscillators that are in a typical non-synchronized state.

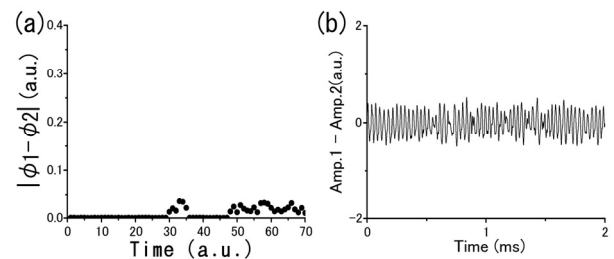


Fig. 7. Correlation between two oscillators is shown: (a) the phase difference  $|\phi_1 - \phi_2|$  and (b) amplitude difference between two oscillators that are in a typical synchronized state.

Thus, there is no correlation between the phases, and the two waves are not phase synchronized. Figure 6(b) shows that the oscillation of the amplitude difference is almost disorder. Thus, there is no correlation between amplitudes, and the two waves are not synchronized with respect to their amplitudes. Figures 7(a) and (b) show the phase difference between two oscillators and their amplitude difference, respectively, when the oscillators are in the

typical synchronized state. Sampled time series are analyzed using the same low-pass filter. Figure 7(a) shows that the phase difference between the two coupled oscillators remains practically constant at approximately zero with time. Thus, the phases of the coupled oscillators are synchronized in the process of coupling. Figure 6(b) shows that the oscillation of the amplitude difference is almost order. Thus, there exists a correlation between amplitudes, and the amplitudes of the two waves are synchronized.

#### 4. Conclusion

The dynamical behavior of coupled spatially extended systems, caused by current-driven ion-acoustic instability, is investigated experimentally. When two waves interact, and the control parameter governing either of the two systems is varied gradually, the systems exhibit synchronization in a certain region. It is found that the coupled systems exhibit hysteresis phenomena around the threshold of synchronization, account of the strong nonlinearity of plasma. When synchronization occurs in coupled oscillators, the two oscillators possess correlation with respect to both their phase and amplitude.

#### References

- [1] C. Hugenii, *Horoloquim Oscillatorium* (Parisiis, France, 1673).
- [2] H. Fujisaka and T. Yamada, *Prog. Theor. Phys.* **69**, 32 (1983).
- [3] L. M. Pecora and T. L. Carroll, *Phys. Rev. Lett.* **64**, 821 (1990).
- [4] K. Coffman, W. D. McCormick, and Harry L. Swinney, *Phys. Rev. Lett.* **56**, 999 (1986).
- [5] R. Roy and K. S. Thornburg, Jr, *Phys. Rev. Lett.* **72**, 2009 (1994).
- [6] H. Yamazaki, T. Yamada, and S. Kai, *Phys. Rev. Lett.* **81**, 4112 (1998).
- [7] T. Fukuyama and Y. Kawai, *J. Phys. Soc. Jpn.* **71**, 1809 (2002).
- [8] T. Winfree, *J. Theor. Biol.* **16**, 15 (1967).
- [9] S. Boccaletti, J. Bragard, F. T. Arecchi, and H. Mancini, *Phys. Rev. Lett.* **83**, 536 (1999).
- [10] N. Baba, A. Amann, E. Schoell, and W. Just, *Phys. Rev. Lett.* **89**, 074101 (2002).
- [11] R. Neubecker and B. Guetlich, *Phys. Rev. Lett.* **92**, 154101 (2004).
- [12] T. Fukuyama, R. Kozakov, H. Testrich, and C. Wilke, *Phys. Rev. Lett.* **96**, 024101 (2006).
- [13] M. G. Rosenblum, A. S. Pikovsky, and J. Kurths, *Phys. Rev. Lett.* **78**, 4193 (1997).
- [14] M. G. Rosenblum, A. S. Pikovsky, and J. Kurths, *Phys. Rev. Lett.* **76**, 1804 (1996).
- [15] T. Fukuyama and Y. Kawai, *J. Phys. Soc. Jpn.* **71**, 1809 (2002).
- [16] R. J. Taylor, K. R. Mackenzie and H. Ikezi: *Rev. Sci. Instrum.* **43**, 1675 (1972).
- [17] K. Taniguchi, H. Kuwae, N. Hayashi, and Y. Kawai, *Phys. Plasmas* **5**, 401 (1998).
- [18] M. Yamada and M. Raether, *Phys. Fluids* **18**, 361 (1975).
- [19] K. Nishikawa and C.-S. Wu, *Phys. Rev. Lett.* **23**, 1020 (1969).
- [20] D. B. Fenneman, M. Raether, and M. Yamada, *Phys. Fluids* **16**, 871 (1973).
- [21] D.-I. Choi and W. Horton, Jr, *Phys. Fluids* **17**, 2048 (1974).
- [22] H. Tanaca, A. Hirose, and M. Koganei, *Phys. Rev.* **161**, 94 (1967).
- [23] Y. Kawai, Ch. Hollenstein, and M. Guyot, *Phys. Fluids* **21**, 970 (1978).